CLIMATOLOGY

The lightness of water vapor helps to stabilize tropical climate

Seth D. Seidel[1,2] and Da Yang[1,2]*

Moist air is lighter than dry air at the same temperature, pressure, and volume because the molecular weight of water is less than that of dry air. We call this the vapor buoyancy effect. Although this effect is well documented, its impact on Earth's climate has been overlooked. Here, we show that the lightness of water vapor helps to stabilize tropical climate by increasing the outgoing longwave radiation (OLR). In the tropical atmosphere, buoyancy is horizontally uniform. Then, the vapor buoyancy in the moist regions must be balanced by warmer temperatures in the dry regions of the tropical atmosphere. These higher temperatures increase tropical OLR. This radiative effect increases with warming, leading to a negative climate feedback. At a near present-day surface temperature, vapor buoyancy is responsible for a radiative effect of 1 W/m^2 and a negative climate feedback of about 0.15 W/m^2 per kelvin.

INTRODUCTION

Geological evidence suggests that tropical sea surface temperature (SST) varies considerably less than higher-latitude SST (*1*–*4*). Although this geological evidence reflects a wide range of uncertainty, the consensus is that tropical climate is more stable than extratropical climate. This local climate stability in the tropics has global implications. Global climate warming results in greater warming at the poles than in the tropics, weakening the meridional temperature gradient (*5*). This would alter the general circulation of the atmosphere. Past work has considered how the temperature gradient would decline with warming through the polar amplification of climate warming, caused by polar-region feedbacks (*5*–*7*) or enhanced poleward energy transport (*8*, *9*). Instead, we propose a low-latitude feedback that leads to tropical damping by emitting more energy to space with warming.

Tropical climate stability may be explained by negative climate feedbacks, which, in a warming climate, cause additional outgoing longwave radiation (OLR) or reduced shortwave absorption by the Earth system. Previous studies have explored such feedback mechanisms. Lindzen *et al.* (*10*) proposed that increased SST in the tropics would result in reduced cirrus clouds, leading to enhanced OLR from Earth's atmosphere. Studies have also proposed that the ability of atmospheric circulations to transport energy and create dry, emissive regions is key to regulate tropical climate (*8*, *11*). More recent studies have considered convection's tendency to aggregate more in warmer climates, yielding broader and drier clear-sky regions, efficiently emitting longwave radiation to space (*12*–*14*). However, each of these mechanisms is currently subject to considerable uncertainties in a warming climate (*15*, *16*).

Here, we offer a different explanation of the tropics' climate stability by way of a robust clear-sky feedback. The magnitude of this feedback may be estimated with greater certainty than for feedbacks depending on changes in clouds and circulation. In a recent paper, Yang and Seidel (*17*) proposed a clear-sky vapor buoyancy feedback that stabilizes tropical climate. Using a semianalytical model, the authors estimated that the radiative effect is about 2 to 4 W/m^2 and that the feedback parameter is about 0.2 W/m^2 per kelvin, which seem to be substantial for Earth's climate. The authors further suggested that this effect exponentially increases with climate warming, so it could effectively stabilize tropical climate at higher temperatures. However, because of their theoretical approach, the key ingredients of the feedback are assumed or even imposed, as opposed to self-emerging in the model. For example, they imposed a weak buoyancy gradient (WBG) in the tropical free troposphere, rather than explicitly simulating it in the model. The magnitude of the proposed feedback critically depends on water vapor's distribution in the tropical atmosphere, which was also not explicitly represented. Here, we will explicitly simulate atmospheric circulations and water vapor distributions using a cloud- model (CRM). CRMs have a typical grid spacing of *O* (1 km) and can adequately simulate deep convective storms. In our numerical experiments, an atmosphere with weak horizontal buoyancy gradient and realistic water vapor distribution will self-emerge. This paper will show that the lightness of water vapor has a profound impact on Earth's energy balance and climate stability.

Vapor buoyancy feedback

The "recipe" for the proposed mechanism requires three key ingredients: (I1) large-scale circulations that organize the tropics into comparatively moist and dry regions (*11*), (I2) a weak horizontal buoyancy gradient (WBG) (*18*–*20*), and (I3) the vapor buoyancy effect itself. While each of these ideas has a long history, the novelty of our proposal lies in their synthesis.

(I1) The tropical atmosphere is organized into comparatively moist and dry regions by large-scale circulations, e.g., the Hadley and Walker circulations (Fig. 1A). The ascending branches of these circulations are characterized by ubiquitous deep convection (thunderstorms) and high relative humidity (RH). There, the atmosphere is opaque to longwave radiation and may approach a local runaway greenhouse state, in which OLR remains roughly constant with surface warming (*11*, *21*). The descending branches are characterized by clear skies and low RH. The circulations transport energy from the moist region to the dry region, where longwave radiation is emitted from Earth's atmosphere. While much of the subtropics are part of such a dry region associated with the subsiding branch of the Hadley circulations, even large parts of the deep tropics can be characterized by dry, subsiding air due to east-west atmospheric circulations, such as the Walker circulation. Because the moist

[1]University of California, Davis, Davis, CA, USA. [2]Lawrence Berkeley National Laboratory, Berkeley, CA, USA.
*Corresponding author. Email: dayang@ucdavis.edu

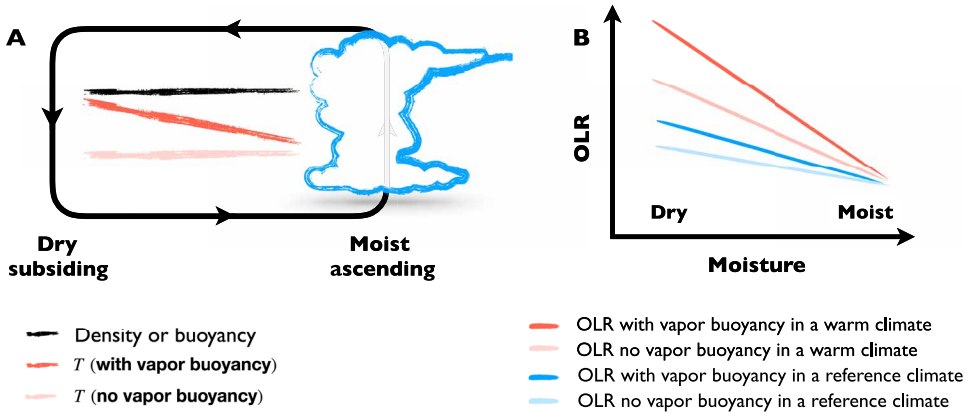

Fig. 1. Proposed mechanism of the vapor buoyancy feedback. (**A**) The atmosphere is organized into moist and dry regions, with the dry region being responsible for most of the atmosphere's OLR. In an atmosphere with vapor buoyancy, the WBG necessitates a warmer dry region than if there were no vapor buoyancy effect, which increases OLR. (**B**) The expected dependence of OLR on column water vapor according to our hypothesis. We expect there to be little difference in the OLR originating from the moist regions, but the vapor buoyancy effect will yield greater OLR in the dry region. We expect this OLR difference to be greater in warmer climates. This constitutes a negative climate feedback.

region's OLR is relatively insensitive to surface warming, it is the properties of the dry region—its temperature, water vapor profiles, and spatial area—that primarily determine the tropics' OLR and how OLR responds to climate forcings.

(I2) We are interested in the atmospheric temperature in the dry region and thereby in how buoyancy is distributed in the tropical atmosphere. Buoyancy is an upward force by virtue of the density difference between an air parcel and the surrounding environment. In Earth's atmosphere, buoyancy is determined by its temperature and water vapor mixing ratio (kg/kg). We shall use this relationship between buoyancy, temperature, and water vapor content to understand the dry-region temperature profile. The WBG approximation simplifies the dynamics of the tropical free troposphere by assuming buoyancy to be horizontally homogeneous. In the tropics, the effect of planetary rotation is comparatively small, so gravity waves can effectively smooth out horizontal buoyancy anomalies (*18*–*20*). Sometimes, this is further simplified to the weak temperature gradient approximation, which assumes that water vapor has a negligible effect on buoyancy. However, for our purposes, we must be more precise.

(I3) The vapor buoyancy effect, also known as the virtual effect, accounts for how the molecular weight of water vapor influences the buoyancy of moist air. Water vapor has a molecular mass of 18 g/mol, considerably less than the mass of dry air at 29 g/mol. A parcel of moist air is lighter and more buoyant than a parcel of dry air at the same temperature and pressure. To capture this effect, we use virtual temperature to represent buoyancy

$$T_v = T\left(\frac{1 + r/\epsilon}{1 + r}\right) \quad (1)$$

T is the parcel's temperature (K), r is its water vapor mixing ratio (kg/kg), and $\epsilon = M_v/M_d$, where M_v and M_d are the average molecular mass of water vapor and dry air, respectively.

The above ingredients produce the vapor buoyancy feedback (Fig. 1). In the tropical atmosphere, the temperature profile of the moist region is set by convective storms, and temperature must increase toward the dry region, balancing reduced vapor buoyancy according to WBG (dark red line in Fig. 1A). This makes the dry region warmer than it otherwise would be in the absence of vapor buoyancy (light red line in Fig. 1A). The greater temperature leads to more OLR. This is a negative radiative effect, and its magnitude depends on the humidity contrast between the moist and dry regions (Fig. 1B). Assuming that RH remains the same, the specific humidity contrast increases with warming, leading to a larger horizontal temperature difference and thereby a stronger radiative effect of vapor buoyancy in a warmer climate (Fig. 1B). This is thus a negative feedback, stabilizing the climate.

The vapor buoyancy feedback represents a substantial departure from the current understanding of the tropical lapse rate feedback, in which latent heating causes the moist adiabatic lapse rate to decline with climate warming (*22*). The upper troposphere warms more than the surface, increasing OLR. That process can be represented in a single column. However, the origin and amplitude of the vapor buoyancy feedback depend on horizontal distributions of temperature and moisture. Understanding the vapor buoyancy feedback, therefore, requires at least two columns (*17*) or even two dimensions as in this study.

We make three predictions according to this theory:

(P1) There is a substantial horizontal temperature gradient in the lower free troposphere where WBG is effective and where water vapor is abundant (Fig. 1A).

(P2) The vapor buoyancy effect increases OLR (Fig. 1).

(P3) The strength of this effect increases with surface temperature (Fig. 1B).

RESULTS

We test the vapor buoyancy feedback using two-dimensional (2D) cloud-resolving simulations of idealized overturning circulations with identifiable moist and dry patches. We perform these numerical simulations over a wide range of SSTs. At a given SST, we perform two simulations: a control simulation with the vapor buoyancy effect, and a mechanism-denial simulation without the vapor buoyancy effect. This pair of simulations highlights the effect of vapor buoyancy. A similar approach has been widely used, e.g., to study the radiative effect of clouds in climate models. To implement the idealized circulations, we use convective self-aggregation, a phenomenon in which an atmosphere under uniform boundary conditions spontaneously develops a large-scale overturning circulation with an ascending

region characterized by deep convection and a subsiding region characterized by anomalously dry conditions (*23*–*27*). Convective self-aggregation is particularly suitable for investigating the vapor buoyancy feedback because its steady overturning circulation has discernible, persistent moist and dry regions. The model setup for these simulations is discussed in Methods.

Convective self-aggregation is successfully simulated in a wide range of climates. Figure 2 shows the evolution of precipitable water (PW) over space and time at different SSTs, without and with the vapor buoyancy effect. Notably, the horizontal scale of self-aggregation depends on the temperature and the presence of the vapor buoyancy effect. Yang (*28*) showed that the vapor buoyancy effect is responsible for the scale of self-aggregation. This is because the horizontal scale is principally determined by the horizontal mass flux within the boundary layer, which is, in turn, determined by the boundary layer density gradient. In a self-aggregated boundary layer, most of the density differences across the domain arise mainly because of vapor buoyancy, rather than to temperature buoyancy. Therefore, by removing the vapor buoyancy effect, we have also removed a principal scale-setting mechanism.

Prediction 1: A substantial temperature gradient

Figure 3 shows that the vapor buoyancy effect is responsible for substantial temperature gradients in the lower free troposphere. The horizontal axis is the percentile rank of PW, the sorting method for which is covered in Methods. The red lines are absolute temperature contours (isotherms), and the black lines are virtual temperature contours (isopycnals). Both atmospheres exhibit negligible horizontal gradients in buoyancy, but there is a considerable temperature gradient in the control atmosphere with vapor buoyancy, which has also been observed in the real tropical atmosphere (*17*). The temperature profiles are nearly identical in the moist region of either atmosphere, but they diverge toward the dry regions: The vapor buoyancy effect warms the lower free troposphere in the dry region. Comparing the 90th percentile column to the 10th percentile column in the 300-K simulation, the temperature difference peaks at 1.7 K, at a pressure level of 872 hPa. Given that this difference is not present in the mechanism-denial simulations where water vapor does not affect buoyancy, we can attribute this warming to the vapor buoyancy effect.

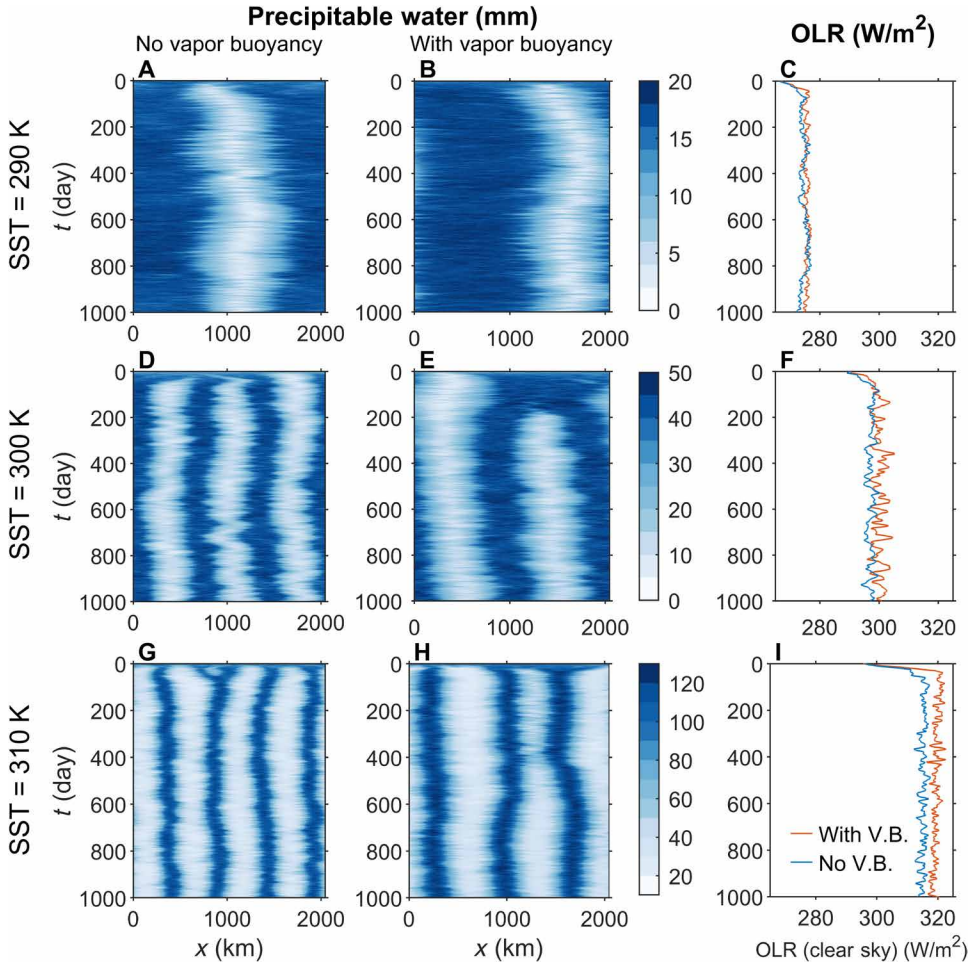

Fig. 2. Simulated water vapor fields and OLR in different climates. (**A**, **B**, **D**, **E**, **G**, and **H**) Precipitable water over time, showing convective self-aggregation. During the course of a simulation, the atmosphere organizes into distinct moist and dry regions despite the uniform boundary conditions. Deep convection occurs almost exclusively in the moist regions, while clear skies and low humidity characterize the dry region. (**C**, **F**, and **I**) A 10-day moving average of clear-sky OLR. Once a distinct dry region develops in each simulation, the atmosphere with vapor buoyancy (V.B.) exhibits greater radiative cooling.

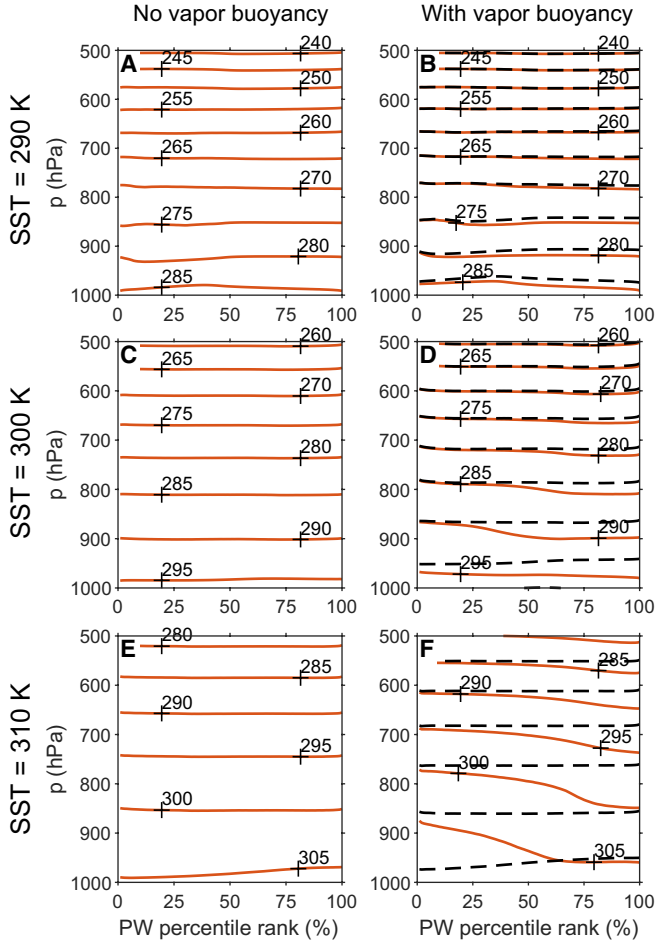

Fig. 3. Temperature and virtual temperature fields as organized by column PW. Red contours correspond to absolute temperature (isotherms), and black contours correspond to virtual temperature (i.e., density) for the pair of simulations with (**A** and **B**) SST = 290 K, (**C** and **D**) SST = 300 K, and (**E** and **F**) SST = 310 K. The temperature profile is nearly identical in the moist region of either atmosphere. The virtual temperature gradient is weak in the free troposphere, warming the dry columns when the vapor buoyancy effect is turned on.

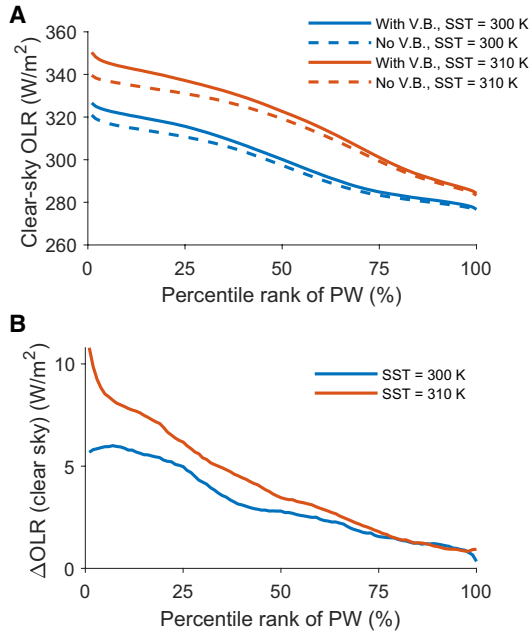

Fig. 4. Simulated difference in OLR. (**A**) Relationship between clear-sky OLR and the percentile rank of PW, with and without the vapor buoyancy effect. There are similar values for OLR in the moist region, but the with-vapor-buoyancy atmosphere emits greater OLR in the dry region, consistent with the prediction in Fig. 1B. (**B**) Increase in OLR from adding the vapor buoyancy effect.

Prediction 2: The vapor buoyancy effect increases OLR

We shall compare the two—control and mechanism-denial—simulations at SST = 300 K, showing that the vapor buoyancy effect increases OLR at a given PW rank and that the vapor buoyancy effect increases the domain-average OLR by warming the lower troposphere of the dry, subsiding region. We focus on the clear-sky OLR diagnostics because our prediction is based on clear-sky radiation and because the all-sky and clear-sky OLR increases are of similar magnitudes (see text S1 for a discussion of clouds and their influence on radiation in these simulations). Using the same column-sorting approach as for Fig. 3, we have calculated clear-sky OLR's dependence on PW. Figure 4A shows that the vapor buoyancy effect enhances clear-sky OLR. The strength of this effect is near zero in the moistest columns but increases gradually toward the driest columns. This is consistent with the prediction presented in Fig. 1B. The time series of domain-mean OLR is shown in Fig. 2. As the atmospheres self-aggregate, OLR in the control experiment exceeds that in the mechanism-denial experiment, and this difference persists. Averaged over the last 750 days of simulation, this effect accounts for a 3.1 W/m^2 increase in OLR in the Earth-like reference climate with SST = 300 K. Compared with the 4 W/m^2 direct radiative forcing associated with the doubling atmospheric CO_2, vapor buoyancy's influence on OLR is quite profound.

Prediction 3: The strength of this effect increases with SST

Figure 4A shows clear-sky OLR for the control and mechanism-denial simulations for 300- and 310-K SSTs. The gap in clear-sky OLR between the two simulations is greater in the SST = 310-K simulation pair. Figure 4B shows this more clearly, depicting the difference in clear-sky OLR in either pair of simulations. This confirms the prediction in Fig. 1B.

To see the domain-mean differences in OLR, we refer first to the time series in Fig. 2. The difference in domain-mean OLR increases with SST. Figure 5A depicts the domain- and time-averaged change in clear-sky OLR due to vapor buoyancy across a wide range of climates

$$\Delta OLR = OLR_v - OLR_{nv} \quad (2)$$

where v and nv denote the control (with vapor buoyancy) and mechanism-denial simulations (no vapor buoyancy), respectively. As shown in Fig. 5A, ΔOLR is 3.1 W/m^2 when SST = 300 K and 4.1 W/m^2 when SST = 310 K. ΔOLR generally increases with SST, acting as a negative climate feedback. If a perturbation was to warm the climate, the vapor buoyancy effect would counteract that by increasing OLR. However, the signal in Fig. 5A results from a combination of factors, including the vapor buoyancy feedback, changes in water vapor distribution, and others, so ΔOLR does not increase

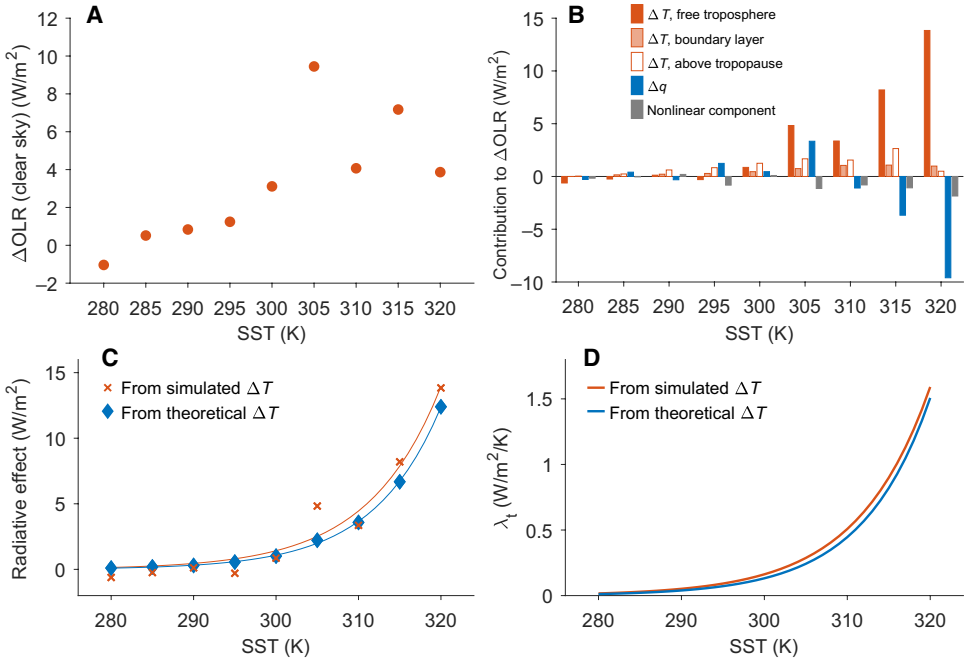

Fig. 5. Feedback analysis. (**A**) Increase in clear-sky OLR from adding the vapor buoyancy effect. Because radiative cooling increases with SST, this constitutes a negative climate feedback. (**B**) Domain-averaged Δ*OLR* decomposed into components due to the linear effects of both temperature and water vapor. The temperature contribution is split into free troposphere, boundary layer, and above-tropopause components. The boundary layer top was assumed at 900 hPa. Tropopause was identified as the lowest level where domain- and time-averaged radiative heating is approximately zero in the simulation with vapor buoyancy. The nonlinear component is calculated as the residual of the Δ*OLR* from the simulations. The free-troposphere temperature component contains the proposed vapor buoyancy radiative effect. (**C**) The marks represent the radiative effect, which is calculated by multiplying the temperature radiative kernel by the Δ*T* profiles. The curves represent exponential fits to the marks. (**D**) The total feedback parameter λ_t, calculated on the basis of the exponential fits, shows the strength of the vapor buoyancy feedback.

monotonically with surface temperature. To separate these effects from one another, we perform radiative kernel calculations.

Components of Δ*OLR*

We use radiative kernels to quantify the share of Δ*OLR* that results from changes in both temperature and water vapor, respectively, between the control and mechanism-denial simulations (refer to Methods for a description of the radiative kernels and how they are applied to the simulation data). The kernels themselves are presented in text S2. Figure 5B shows the result of the kernel analysis, which is a linear decomposition of Δ*OLR* into its components due to the differences in the temperature and moisture fields between the two simulations at a given SST.

The proposed radiative effect of vapor buoyancy results from the free-troposphere temperature difference, Δ*T*, between the control simulation and the mechanism-denial simulation (the left column in Fig. 6). The free troposphere lies between the boundary layer top and the tropopause. We take p_{bl} = 900 hPa as the boundary layer top. Considering the tropopause as the radiative-convective boundary, we have identified it where radiative cooling rate is approximately zero. Text S3 shows the radiative cooling profiles and the calculated tropopause level. The free-troposphere temperature component of Δ*OLR* is an estimate of the radiative effect of vapor buoyancy (dark red bars in Fig. 5B). Because the water vapor field is held constant when applying the temperature kernel, this estimate holds the area of the dry, subsiding region as constant between simulations. Therefore, the calculated OLR difference is only due to temperature changes. This method estimates the radiative effect as about 0.9 W/m^2 at 300-K SST. This increases to about 14 W/m^2 at 320-K SST, suggesting a robust negative climate feedback mechanism in the atmosphere with vapor buoyancy. Text S4 reproduces this calculation assuming a higher boundary layer top of p_{bl} = 800 hPa, showing that the analysis is robust to the location of the boundary layer top.

The linear component of Δ*OLR* associated with differences in water vapor contributes substantially (blue bars in Fig. 5B). This result suggests that water vapor distribution changes when we switch off the vapor buoyancy effect, which is not considered in the simple model developed by Yang and Seidel (*17*). The water vapor contribution to Δ*OLR* reinforces the radiative effect of vapor buoyancy around the reference climate but counteracts it in warmer climates, lacking a robust trend with SST. Understanding this behavior would require us to study how vapor buoyancy affects the water vapor distribution, which is beyond the scope of this paper. We have also computed the boundary-layer contributions to Δ*OLR* and find that the effect is negligible. The temperature above tropopause is a positive component of Δ*OLR*, possibly because the stratosphere is in radiative balance with a warmer troposphere in the control simulations. This stratosphere component is substantial in the reference climate but quickly becomes much smaller relative to the free-troposphere component with climate warming. Here, we do not consider this as part of the radiative effect of vapor buoyancy, as WBG dynamics do not apply in the stratosphere. This simplification will not affect the overall estimate of the feedback parameter because the increasing trend of the radiative effect is dominated by the free-troposphere component. The vapor buoyancy feedback is mainly a free-troposphere feedback process. The nonlinear term is

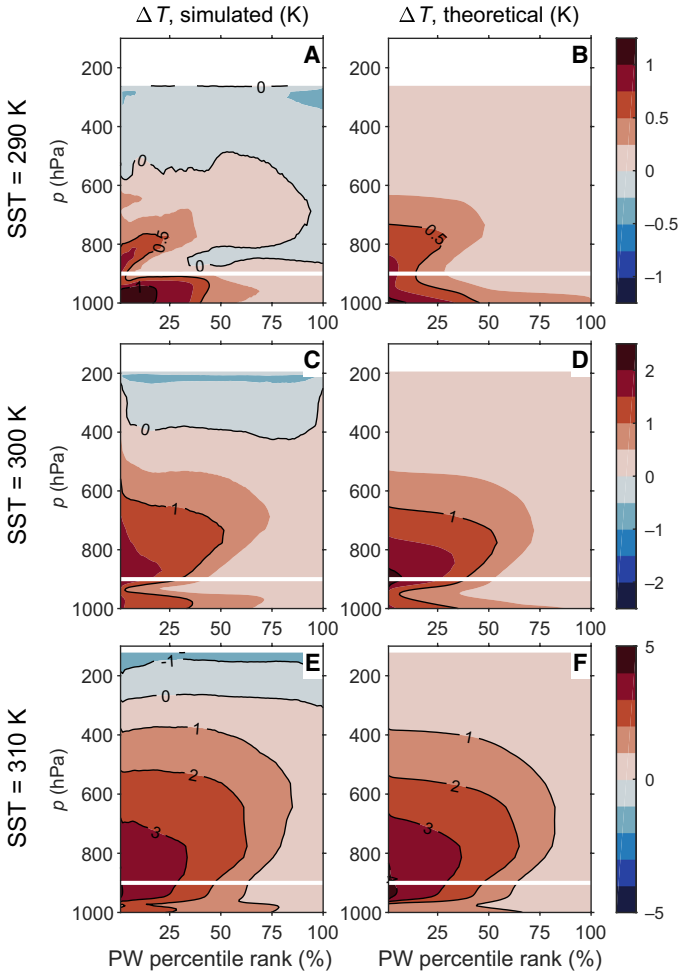

Fig. 6. Temperature difference due to vapor buoyancy. (**A**, **C**, and **E**) ΔT is the additional temperature due to the vapor buoyancy effect as calculated by subtracting the temperature profiles of the simulations with and without the vapor buoyancy effect. That is, we subtract the left-hand panels of Fig. 3 from the right-hand panels. (**B**, **D**, and **F**) ΔT as calculated from a single simulation using Eq. 4. The white lines denote the 900-hPa level we use for the boundary layer top. We do not show values of ΔT above the tropopause, where WBG no longer applies.

the residual of the linear decomposition. The smallness of that residual supports the approximate linearity of the problem, which is necessary for the radiative kernel analysis.

Estimating the radiative effect from a single atmosphere

So far, we have estimated the radiative effect of vapor buoyancy by simulating two different atmospheres: the control atmosphere (with vapor buoyancy) and the mechanism-denial atmosphere (without vapor buoyancy). Now, we will develop another method to estimate ΔT and its associated radiative effect from only the control atmosphere. This approach will demonstrate that the simulated effect arises because of the robust physics we propose, as opposed to model details. This new calculation of ΔT will also show how to estimate the radiative effect of vapor buoyancy using either observations or comprehensive climate models.

According to WBG, we assume that the buoyancy of any air parcel is set by convective plumes with RH = 100%. The temperature difference ΔT due to vapor buoyancy is calculated as the difference between the temperature of the observed or simulated atmosphere and the temperature of convective plumes with equal density

$$T_{\mathrm{m}}\left(\frac{1+r_{\mathrm{m}}^{*}/\epsilon}{1+r_{\mathrm{m}}^{*}}\right)=T\left(\frac{1+r/\epsilon}{1+r}\right) \tag{3}$$

where T is the observed temperature of the dry parcel, r is the observed water vapor mixing ratio (kg/kg), $T_m = T - \Delta T$ is the temperature of the convective plume, and $r_{\mathrm{m}}^{*} = r_{\mathrm{m}}^{*}(T_{\mathrm{m}}, p)$ is the saturation mixing ratio of the moist parcel. We rearrange Eq. 3 using the relationship $T_{\mathrm{m}} = T - \Delta T$

$$\Delta T=T\left(\frac{1+r_{\mathrm{m}}^{*}(T_{\mathrm{m}},p)/\epsilon}{1+r_{\mathrm{m}}^{*}(T_{\mathrm{m}},p)}-\frac{1+r/\epsilon}{1+r}\right)\left(\frac{1+r_{\mathrm{m}}^{*}(T_{\mathrm{m}},p)}{1+r_{\mathrm{m}}^{*}(T_{\mathrm{m}},p)/\epsilon}\right) \tag{4}$$

We have chosen this precise form of ΔT, without approximations, as analytical tractability is unnecessary here. On the right-hand side, the values of T and r are both known. These are the properties of the observed or simulated air parcel. However, r_{m}^{*} is a function of T_{m} and therefore a function of ΔT. ΔT cannot be readily isolated to one side of the equation without further approximation. Therefore, we solve Eq. 4 iteratively. We use the Newton-Raphson method, with the derivative approximated numerically, ending the iteration when the correction is less than 10^{-3} K.

The right column in Fig. 6 shows this theoretical calculation of ΔT, applying Eq. 4 to the control simulation data. In the lower troposphere, the magnitude and structure of ΔT are both remarkably similar between the two methods, indicating that Eq. 4 appropriately captures the warming due to the vapor buoyancy effect. This correspondence breaks down near the tropopause: The simulation results show that the atmosphere is slightly cooler with vapor buoyancy. This difference has little impact on the radiative effect calculation, as we show below. We have also included in text S5 an alternate calculation of ΔT, which does not require a presumed moist parcel and instead uses data from the moistest columns in the simulations. That calculation agrees with the results presented here.

We calculate the radiative effect of vapor buoyancy by applying the temperature radiative kernels to the theoretical calculation of ΔT for each simulation with vapor buoyancy. As before, we only use data from the free troposphere. Figure 5C shows the results of this new, theoretical calculation of the radiative effect of vapor buoyancy alongside the previous calculation. The simulation-pair marks in Fig. 5C are simply a reproduction of the free-troposphere temperature component in Fig. 5B. The results show that the radiative effect exponentially increases with SST, which is likely because ΔT increases with SST exponentially (*17*). The two fitted curves correspond well in both magnitude and trend. Thus, the temperature and vapor profiles of a single, with-vapor-buoyancy atmosphere are sufficient to estimate the strength of the radiative effect of vapor buoyancy.

Feedback parameter

Last, it is useful to calculate a feedback parameter—the amount by which the radiative effect increases per unit surface warming. We define the feedback parameter as

$$\lambda_{\mathrm{t}}=\frac{dR_{vb}}{dSST} \tag{5}$$

where R_{vb} is the radiative effect of vapor buoyancy. λ_t measures the total sensitivity of the radiative effect of vapor buoyancy to SST. λ_t results from a combination of changes with climate warming in both ΔT and the atmosphere's base state (water vapor and temperature profiles). Yang and Seidel (*17*) calculated λ_{vb}, which isolates only the change in R_{vb} due to the change in ΔT, and found that it has a similar magnitude as λ_t. Figure 5D shows λ_t based on the fitted exponential curves in Fig. 5C. In the Earth-like reference climate, we estimate λ_t to be 0.16 and 0.13 W/m^2 per kelvin for the simulation-pair and theoretical calculations of ΔT, respectively. Following our assumption of an exponential trend in R_{vb}, λ_t also increases exponentially with climate warming, achieving a magnitude of about 1.5 W/m^2 per kelvin at 320 K. This compares to the Planck feedback, a leading-order longwave feedback that results from a uniform warming of the atmosphere. The Planck feedback is about 4.6 W/m^2 per kelvin at that temperature. The vapor buoyancy feedback reaches one-third of that magnitude. In such warm climates, the vapor buoyancy feedback may be of primary importance for climate stability of Earth and other terrestrial planets. These climates are much more stable than what has been recognized in the past studies that ignored the vapor buoyancy effect (*11*, *29*).

DISCUSSION

This paper tests the hypothesis that the vapor buoyancy effect stabilizes Earth's climate in the tropics. Using 2D CRM simulations, we have demonstrated that the radiative effect of vapor buoyancy is approximately 1 W/m^2 in the reference climate, a value comparable to the direct radiative forcing due to doubling atmospheric CO_2. Our calculations suggest that this radiative effect exponentially increases with climate warming. This effect results in a negative feedback of around 0.15 W/m^2 per kelvin in the reference climate, which is of the same order of magnitude as the net cloud feedback and surface albedo feedback (*16*, *22*).

Contemporary cloud-resolving and general circulation models have the physics necessary to simulate the vapor buoyancy feedback. Therefore, the feedback should be reflected in past model-based assessments of climate sensitivity. However, simulation does not entail understanding. This study explains how the vapor buoyancy feedback occurs and presents evidence that it helps to shape Earth's tropical climate. Other authors have aggregated all greater-than-surface warming of the troposphere together into a single "lapse rate feedback" (*22*, *30*). Such a combined approach may not be appropriate. The origin and amplitude of the vapor buoyancy feedback depend on the horizontal distributions of temperature and moisture. Understanding the vapor buoyancy feedback, therefore, requires at least two columns or even two dimensions. This is fundamentally different from the conventional explanation of the tropical lapse rate feedback based on a single-column process—the temperature profile (the moist adiabat) is steepening from additional latent heating with warming.

Single-column models are widely used to simulate clouds and climate both on Earth and other planets (*29*). These models simulate a representative atmospheric column, usually in a radiative-convective equilibrium state. Such a model is not able to represent the vapor buoyancy feedback, which requires at least two columns, and would underestimate climate stability. This deficiency reinforces past arguments in favor of using two-column models, which represent the two branches of an overturning circulation (*11*, *31*). In such a model, the column processes, such as convection, may be either parameterized or explicitly simulated. However, the effects of large-scale dynamics are always parameterized, often by imposing a weak horizontal temperature gradient: The two columns have equal temperatures (*31*, *32*). Such an assumption precludes the vapor buoyancy feedback. By excluding the vapor buoyancy effect, these modeling frameworks have considerable biases in estimating atmospheric buoyancy, cloud fraction, radiative feedbacks, and, thereby, climate stability. Therefore, it is desirable to properly represent the vapor buoyancy effect when using the column modeling approach.

The vapor buoyancy feedback requires that the atmosphere is organized into large-scale overturning circulations and that there is abundant water vapor. These criteria are best met in Earth's tropics. The strength of this feedback is determined by the magnitude of water vapor differences across the tropics and the relative size of the dry, subsiding regions of the atmosphere. We refer the reader to Bretherton *et al.* (*33*), whose Figure 3B depicts that not only are there very large water vapor differences within the tropics but also a broad dry region to emit OLR. Therefore, the vapor buoyancy feedback may play a profound role in stabilizing Earth's tropical climate at present. We expect that it plays an even greater role in explaining Earth's past climates. A recent review of paleoclimate data and simulations of the hot Eocene climate has suggested surface temperatures as high as 310 K in the tropics (*34*). Although considerably warmer than our present climate, such a temperature still reflects greater stability in tropical climate than in extratropical climate. Referring to our Fig. 5D, such surface temperatures would imply a much stronger vapor buoyancy feedback than at present (about 0.5 W/m^2 per kelvin). Therefore, the vapor buoyancy feedback may have played a leading role in stabilizing tropical climates in the past.

The vapor buoyancy feedback may also stabilize (or destabilize) planetary climates. Several characteristics of a planet may alter the vapor buoyancy feedback:

1. The planetary rotation rate. Many planets rotate more slowly than Earth. Recent work has considered the habitability of tidally locked extrasolar planets with persistent day and night hemispheres. With an orbital period in the tens of Earth days, atmospheric dynamics on such planets would resemble those of Earth's tropics. Rather than altering the meridional temperature gradient, a negative vapor buoyancy feedback on such a planet would effectively expand the inner edge of the habitable zone—the set of orbits where liquid water can exist near the surface.

2. The ratio of the molar mass of vapor to that of dry air (ε). In planetary atmospheres, the molecular weights of dry air and vapor may be notably different from Earth's. The vapor buoyancy effect would be much stronger for water vapor in a carbon dioxide atmosphere. On the other hand, where water vapor is found in a hydrogen atmosphere, the vapor buoyancy effect would be reversed. Then, the proposed vapor buoyancy feedback would also work in reverse, yielding a positive, destabilizing climate feedback.

3. The surface temperature. The feedback strength is remarkably sensitive to surface temperature. It is likely that there are warm terrestrial planets close to the inner edge of their habitable zones. On such planets, the vapor buoyancy feedback more effectively stabilizes the climate than on Earth.

This study uses a 2D CRM with uniform SST. In the 2D CRM simulations, gravity waves, WBG, and water vapor distributions are explicitly simulated, which make this study a meaningful advance beyond Yang and Seidel (*17*). However, there are several limitations due to the idealized approach presented in this paper. For example,

the overturning circulations simulated are due to self-aggregation rather than surface temperature gradients as in Earth's Hadley and Walker circulations. There may be departures from the temperature and water vapor profiles actually observed in the tropics. Therefore, it would be desirable to quantify the vapor buoyancy feedback using comprehensive 3D climate models and observations in future studies. In addition, we have mainly discussed the clear-sky radiative effect in this study. It is also desirable to understand and quantify the cloud effect associated with vapor buoyancy.

METHODS

Cloud-resolving simulations

We simulate convective self-aggregation in a nonrotating 2D atmosphere using the System for Atmospheric Modeling (SAM; version 6.10.8) (*35*). The radiation scheme is that of the National Center for Atmospheric Research (NCAR) Community Atmosphere Model, version 3 (CAM3) (*36*). The microphysics is the SAM one-moment parameterization. The horizontal domain size is 2048 km, and the model top is at 35 km. The horizontal resolution is 2 km. The vertical resolution is 50 m for the lowest 1 km and increases to 600 m above 3 km. A sponge layer occupies the upper 10 km of the model domain. The incoming solar radiation is fixed at 413.9 W/m^2 to match the annual mean insolation on the equator. We fix the SST to a uniform value, and we perform simulations for a wide range of SSTs, from 280 to 320 K. Each simulation is integrated for 1000 days. This paper presents two types of simulations: control simulations with the vapor buoyancy effect and mechanism-denial simulations without the vapor buoyancy effect. We switch off the vapor buoyancy effect by removing the buoyancy dependence on water vapor in the vertical momentum equation, following Yang (*28*). A CRM typically has horizontal grid spacing of *O* (1 km), which is sufficient to resolve deep convective clouds and has been widely used to study tropical convection. However, to fully resolve boundary layer clouds, one would need large eddy simulations with typical horizontal grid spacing of about 50 m. Because our proposed mechanism mainly concerns how vapor buoyancy affects clear-sky temperature profiles in the free troposphere, CRM simulations are sufficient.

Analysis in moisture space

We analyze the model output in PW space. Each simulation contains 1024 columns, integrated over 1000 days, saved in 4-hour intervals. Removing the first 250 days of each simulation, we calculated the 1-day moving mean of the output and then sorted each of the 1024×4500 columns according the percentile rank of PW. We then calculate an average profile at each percentile, yielding 100 percentile–ranked average columns for each simulation. We could instead rank columns according to column RH, but the results presented here are robust to either method. We use the column-sorted data to test the three predictions.

Radiative kernel calculation

We use the CAM radiative transfer model (*36*, *37*) to compute radiative kernels (*38*, *39*). The kernels represent the change in clear-sky OLR with respect to atmospheric temperature profile, or $\frac{\partial \mathrm{OLR}}{\partial T}(p)$ and with respect to the vapor profile, $\frac{\partial \mathrm{OLR}}{\partial q}(p)$. Following the method introduced by Cronin and Wing (*39*), we calculate "approximate" kernels using the PW-sorted columns presented previously. The kernels are based on the control simulations. We calculate each of these partial derivatives by perturbing the temperature or water vapor at a single-model level then running the radiative transfer scheme on both the original and the perturbed atmospheric profiles. We use perturbations of +0.5 K in temperature and −1% in specific humidity to calculate the kernels. The temperature and water vapor radiative kernels for the simulations of 290-, 300-, and 310-K SSTs are presented in text S2.

SUPPLEMENTARY MATERIALS

Supplementary material for this article is available at http://advances.sciencemag.org/cgi/content/full/6/19/eaba1951/DC1

REFERENCES AND NOTES

1. J. Frieling, H. Gebhardt, M. Huber, O. A. Adekeye, S. O. Akande, G. J. Reichart, J. J. Middelburg, S. Schouten, A. Sluijs, Extreme warmth and heat-stressed plankton in the tropics during the paleocene-eocene thermal maximum. *Sci. Adv.* **3**, e1600891 (2017).
2. D. Evans, N. Sagoo, W. Renema, L. J. Cotton, W. Müller, J. A. Todd, P. K. Saraswati, P. Stassen, M. Ziegler, P. N. Pearson, P. J. Valdes, H. P. Affek, Eocene greenhouse climate revealed by coupled clumped isotope-Mg/Ca thermometry. *Proc. Natl. Acad. Sci. U.S.A.* **115**, 1174–1179 (2018).
3. P. N. Pearson, B. E. van Dongen, C. J. Nicholas, R. D. Pancost, S. Schouten, J. M. Singano, B. S. Wade, Stable warm tropical climate through the Eocene Epoch. *Geology* **35**, 211–214 (2007).
4. C. R. Keating-Bitonti, L. C. Ivany, H. P. Affek, P. Douglas, S. D. Samson, Warm, not super-hot, temperatures in the early Eocene subtropics. *Geology* **39**, 771–774 (2011).
5. V. Masson-Delmotte, M. Schulz, A. Abe-Ouchi, J. Beer, A. Ganopolski, J. F. González Rouco, E. Jansen, K. Lambeck, J. Luterbacher, T. Naish, T. Osborn, B. Otto-Bliesner, T. Quinn, R. Ramesh, M. Rojas, X. Shao, A. Timmermann, J. F. G. Rouco, Chapter 5: Information from paleoclimate archives, in *Climate Change 2013 – The Physical Science Basis: Working Group I Contribution to the Fifth Assessment Report of the Intergovernmental Panel on Climate Change* (Cambridge Univ. Press, 2014), pp. 383–464.
6. M. I. Budyko, The effect of solar radiation variations on the climate of the Earth. *Tellus* **21**, 611–619 (1969).
7. I. Cvijanovic, K. Caldeira, Atmospheric impacts of sea ice decline in CO_2 induced global warming. *Climate Dynam.* **44**, 1173–1186 (2015).
8. M. Cai, Dynamical amplification of polar warming. *Geophys. Res. Lett.* **32**, L22710 (2005).
9. S. Lee, A theory for polar amplification from a general circulation perspective. *Asia-Pacific J. Atmos. Sci.* **50**, 31–43 (2014).
10. R. S. Lindzen, M.-D. Chou, A. Y. Hou, Does the Earth have an adaptive infrared iris? *Bull. Am. Meteorol. Soc.* **82**, 417–432 (2001).
11. R. T. Pierrehumbert, Thermostats, radiator fins, and the local runaway greenhouse. *J. Atmos. Sci.* **52**, 1784–1806 (1995).
12. K. Emanuel, A. A. Wing, E. M. Vincent, Radiative-convective instability. *J. Adv. Model. Earth Syst.* **6**, 75–90 (2014).
13. T. Mauritsen, B. Stevens, Missing iris effect as a possible cause of muted hydrological change and high climate sensitivity in models. *Nat. Geosci.* **8**, 346–351 (2015).
14. S. Bony, B. Stevens, D. Coppin, T. Becker, K. A. Reed, A. Voigt, B. Medeiros, Thermodynamic control of anvil cloud amount. *Proc. Natl. Acad. Sci. U.S.A.* **113**, 8927–8932 (2016).
15. S. Bony, B. Stevens, D. M. W. Frierson, C. Jakob, M. Kageyama, R. Pincus, T. G. Shepherd, S. C. Sherwood, A. Pier Siebesma, A. H. Sobel, M. Watanabe, M. J. Webb, Clouds, circulation and climate sensitivity. *Nat. Geosci.* **8**, 261–268 (2015).
16. O. Boucher, D. Randall, P. Artaxo, C. S. Bretherton, Chapter 7: Clouds and aerosols, in *Climate Change 2013: The Physical Science Basis. Contribution of Working Group I to the Fifth Assessment Report of the Intergovernmental Panel on Climate Change*, T. F. Stocker, D. Qin, G.-K. Plattner, M. Tignor, S. K. Allen, J. Doschung, A. Nauels, Y. Xia, V. Bex, P. M. Midgley, Eds. (Cambridge Univ. Press, Cambridge, 2013), pp. 571–657.
17. D. Yang, S. D. Seidel, The incredible lightness of water vapor. *J. Clim. Rev.* **33**, 2841–2851 (2019).
18. J. G. Charney, A note on large-scale motions in the tropics. *J. Atmos. Sci.* **20**, 607–609 (1963).
19. A. H. Sobel, J. Nilsson, L. M. Polvani, The weak temperature gradient approximation and balanced tropical moisture waves. *J. Atmos. Sci.* **58**, 3650–3665 (2002).
20. X. Huang, H.-W. Chuang, A. Dessler, X. Chen, K. Minschwaner, Y. Ming, V. Ramaswamy, A radiative–convective equilibrium perspective of weakening of the tropical walker circulation in response to global warming. *J. Climate* **26**, 1643–1653 (2013).
21. A. P. Ingersoll, The Runaway greenhouse: A history of water on venus. *J. Atmos. Sci.* **26**, 1191–1198 (1969).

22. G. Flato, J. Marotzke, B. Abiodun, P. Braconnot, S. C. Chou, W. D. Collins, P. Cox, F. Driouech, S. Emori, V. Eyring, C. Forest, P. Gleckler, E. Guilyardi, C. Jakob, V. Kattsov, C. Reason, M. Rummukainen, Chapter 9: Evaluation of Climate Models, in *Climate Change 2013: The Physical Science Basis,* T. F. Stocker, D. Qin, G.-K. Plattner, M. Tignor, S. K. Allen, J. Boschung, A. Nauels, Y. Xia, V. Bex, P. M. Midgley, Eds. (Cambridge Univ. Press, Cambridge, United Kingdom and New York, NY, USA, 2013).
23. C. S. Bretherton, P. N. Blossey, M. Khairoutdinov, An energy-balance analysis of deep convective self-aggregation above uniform SST. *J. Atmos. Sci.* **62**, 4273–4292 (2006).
24. C. J. Muller, I. M. Held, Detailed investigation of the self-aggregation of convection in cloud-resolving simulations. *J. Atmos. Sci.* **69**, 2551–2565 (2012).
25. C. Muller, S. Bony, What favors convective aggregation and why? *Geophys. Res. Lett.* **42**, 5626–5634 (2015).
26. C. E. Holloway, S. J. Woolnough, The sensitivity of convective aggregation to diabatic processes in idealized radiative-convective equilibrium simulations. *J. Adv. Model. Earth Syst.* **8**, 166–195 (2016).
27. D. Yang, Boundary layer diabatic processes, the virtual effect, and convective self-aggregation. *J. Adv. Model. Earth Syst.* **10**, 2163–2176 (2018).
28. D. Yang, Boundary layer height and buoyancy determine the horizontal scale of convective self-aggregation. *J. Atmos. Sci.* **75**, 469–478 (2018).
29. R. K. Kopparapu, R. Ramirez, J. F. Kasting, V. Eymet, T. D. Robinson, S. Mahadevan, R. C. Terrien, S. Domagal-Goldman, V. Meadows, R. Deshpande, Habitable zones around main-sequence stars: New estimates. *Astrophys. J.* **765**, 131 (2013).
30. B. J. Soden, I. M. Held, An assessment of climate feedbacks in coupled ocean–Atmosphere models. *J. Climate* **19**, 3354–3360 (2006).
31. J. Yang, D. S. Abbot, A low-order model of water vapor, clouds, and thermal emission for tidally locked terrestrial planets. *Astrophys. J.* **784**, 155 (2014).
32. T. Schneider, C. M. Kaul, K. G. Pressel, Possible climate transitions from breakup of stratocumulus decks under greenhouse warming. *Nat. Geosci.* **12**, 164–168 (2019).
33. C. S. Bretherton, M. E. Peters, L. E. Back, Relationships between water vapor path and precipitation over the tropical oceans. *J. Climate* **17**, 1517–1528 (2004).
34. M. Pagani, M. Huber, B. Sageman, in *Treatise on Geochemistry* (Elsevier, ed. 2, 2013), vol. 6, pp. 281–304; https://www.sciencedirect.com/science/article/pii/B9780080959757013140.
35. M. F. Khairoutdinov, D. A. Randall, Cloud resolving modeling of the ARM summer 1997 IOP: Model formulation, results, uncertainties, and sensitivities. *J. Atmos. Sci.* **60**, 607–625 (2003).
36. W. D. Collins, P. J. Rasch, B. A. Boville, J. J. Hack, J. R. McCaa, D. L. Williamson, B. P. Briegleb, C. M. Bitz, S. J. Lin, M. Zhang, The formulation and atmospheric simulation of the community atmosphere model version 3 (CAM3). *J. Climate* **19**, 2144–2161 (2006).
37. C. S. Zender, Global climatology of abundance and solar absorption of oxygen collision complexes. *J. Geophys. Res. Atmos.* **104**, 24471–24484 (1999).
38. B. J. Soden, I. M. Held, R. C. Colman, K. M. Shell, J. T. Kiehl, C. A. Shields, Quantifying climate feedbacks using radiative kernels. *J. Climate* **21**, 3504–3520 (2008).
39. T. W. Cronin, A. A. Wing, Clouds, circulation, and climate sensitivity in a radiative-convective equilibrium channel model. *J. Adv. Model. Earth Syst.* **9**, 2883–2905 (2017).

Acknowledgments: We thank M. Khairoutdinov for making the CRM (SAM) available to us. We thank A. Ramírez-Reyes for assistance with the radiation code, D. Feldman and T. Cronin for discussions on radiative transfer, I. Fung for discussions on climate feedbacks, and three anonymous reviewers whose feedback helped improve this manuscript. Computational resources were provided by the Department of Energy National Energy Research Scientific Computing Center (NERSC) at the Lawrence Berkeley National Laboratory. **Funding:** This work was partly supported by the Laboratory Directed Research and Development (LDRD) funding from the Berkeley Lab, provided by the Director, Office of Science, of the U.S. Department of Energy under contract DE-AC02-05CH11231. D.Y. and S.D.S. are also supported by a Packard Fellowship for Science and Engineering. **Author contributions:** D.Y. designed and oversaw the research. S.D.S. performed the research and wrote the manuscript, with editing by D.Y. **Competing interests:** The authors declare that they have no competing interests. **Data and materials availability:** All data needed to evaluate the conclusions in the paper are present in the paper and/or the Supplementary Materials. Data used in producing each figure in the main text can be found at https://ucdavis.box.com/s/q2ex8e18gvzzprmk2qf00icw7xufrduh. Additional data related to this paper may be requested from the authors.

Submitted 12 November 2019
Accepted 18 February 2020
Published 6 May 2020
10.1126/sciadv.aba1951

Citation: S. D. Seidel, D. Yang, The lightness of water vapor helps to stabilize tropical climate. *Sci. Adv.* **6**, eaba1951 (2020).

Science Advances

The lightness of water vapor helps to stabilize tropical climate

Seth D. Seidel and Da Yang

Sci Adv **6** (19), eaba1951.
DOI: 10.1126/sciadv.aba1951